

# The *MUR3* Gene of *Arabidopsis* Encodes a Xyloglucan Galactosyltransferase That Is Evolutionarily Related to Animal Exostosins

Michael Madson,<sup>a,1</sup> Christophe Dunand,<sup>b,1,2</sup> Xuemei Li,<sup>b,1</sup> Rajeev Verma,<sup>b</sup> Gary F. Vanzin,<sup>b,3</sup> Jeffrey Caplan,<sup>b</sup> Douglas A. Shoue,<sup>a</sup> Nicholas C. Carpita,<sup>a</sup> and Wolf-Dieter Reiter<sup>b,4</sup>

<sup>a</sup> Department of Botany and Plant Pathology, Purdue University, West Lafayette, Indiana 47907-1155

<sup>b</sup> Department of Molecular and Cell Biology, University of Connecticut, Storrs, Connecticut 06269

**Xyloglucans are the principal glycans that interlace cellulose microfibrils in most flowering plants. The *mur3* mutant of *Arabidopsis* contains a severely altered structure of this polysaccharide because of the absence of a conserved  $\alpha$ -L-fucosyl-(1→2)- $\beta$ -D-galactosyl side chain and excessive galactosylation at an alternative xylose residue. Despite this severe structural alteration, *mur3* plants were phenotypically normal and exhibited tensile strength in their inflorescence stems comparable to that of wild-type plants. The *MUR3* gene was cloned positionally and shown to encode a xyloglucan galactosyltransferase that acts specifically on the third xylose residue within the XXXG core structure of xyloglucan. *MUR3* belongs to a large family of type-II membrane proteins that is evolutionarily conserved among higher plants. The enzyme shows sequence similarities to the glucuronosyltransferase domain of exostosins, a class of animal glycosyltransferases that catalyze the synthesis of heparan sulfate, a glycosaminoglycan with numerous roles in cell differentiation and development. This finding suggests that components of the plant cell wall and of the animal extracellular matrix are synthesized by evolutionarily related enzymes even though the structures of the corresponding polysaccharides are entirely different from each other.**

## INTRODUCTION

The plant cell wall is composed of cellulose microfibrils interlaced with cross-linking glycans, and this strong network is embedded in a gel matrix of pectic polysaccharides (Carpita and Gibeaut, 1993). This extracellular matrix plays numerous roles in the physical control of expansion growth, the establishment of cell shape, and the structural integrity of the plant body. For most dicot and nongraminaceous monocot plants, the principal glycan that interlaces the cellulose microfibrils is xyloglucan (XyG). This polysaccharide is considered essential for establishing a strong network with cellulose microfibrils that provides a pliable cell wall, which can be remodeled by expansins and XyG endotransglucosylases/hydrolases during growth (Nishitani, 1997; Cosgrove, 2000). XyG has a (1→4)- $\beta$ -D-glucan backbone that permits tight binding to cellulose via hydrogen bonding. In most XyGs, three consecutive glucose residues are substituted by D-xylose in (1→6)- $\alpha$ -linkages, leaving a fourth glucosyl residue

unbranched. Cleavage of XyG with a *Trichoderma viride* endoglucanase, whose activity is restricted to unbranched residues, gives six kinds of oligomeric units that constitute a species-specific profile. In addition to the fundamental Xyl<sub>3</sub>Glc<sub>4</sub> oligomer, called XXXG in a standardized nomenclature (Fry et al., 1993), the other oligomers are five possible permutations formed by the addition of (1→2)- $\beta$ -D-galactosyl residues at the second and/or third xylose residue, to give XLXG, XXLG, and XLLG, and a subsequent addition of (1→2)- $\alpha$ -L-fucose at a specific galactosyl unit, to give XXFG and XLFG (Table 1).

Three major hypotheses for the function of the  $\alpha$ -L-Fuc-(1→2)- $\beta$ -D-Gal-(1→2) disaccharide side group have been proposed. First, computer modeling studies of three-dimensional XyG structures suggest that this side chain straightens the glucan backbone to ease the formation of hydrogen bonds with cellulose microfibrils (Levy et al., 1991, 1997). Second, XyG oligomers containing the fucosylated disaccharide modulate auxin-induced growth in excised sections (York et al., 1984; Fry, 1994), which suggests a role in the regulation of expansion growth. An extension of this hypothesis is that the modulation of auxin-induced growth is accomplished by slowing the rate of transglycosylation (Purugganan et al., 1997).

Considerable progress has been made in the identification of glycosyltransferases involved in the biosynthesis of XyG. XyG fucosyltransferases have been cloned from *Arabidopsis* (Perrin et al., 1999) and pea (Faik et al., 2000), and an enzyme that transfers D-xylose residues to cellopentaose in a (1→6)- $\alpha$ -linkage is likely to be a xylosyltransferase in XyG biosynthesis (Faik

<sup>1</sup> These authors contributed equally to this work.

<sup>2</sup> Current address: Laboratory of Plant Biochemistry and Physiology, University of Geneva, 1211 Geneva 4, Switzerland.

<sup>3</sup> Current address: National Renewable Energy Laboratory, Golden, CO 80401.

<sup>4</sup> To whom correspondence should be addressed. E-mail wdreiter@uconnvm.uconn.edu; fax 860-486-4331.

Article, publication date, and citation information can be found at [www.plantcell.org/cgi/doi/10.1105/tpc.009837](http://www.plantcell.org/cgi/doi/10.1105/tpc.009837).

**Table 1.** Oligosaccharide Content of Wild-Type and *mur3* XyG (mol %) Based on Electrospray MS

| Oligosaccharide | Structure | Wild type | <i>mur3</i> |
|-----------------|-----------|-----------|-------------|
| XXXG            |           | 45        | 55          |
| XLXG            |           | 3         | 45          |
| XXLG            |           | 8         | ND          |
| XXFG            |           | 24        | ND          |
| XLLG            |           | 4         | ND          |
| XLFG            |           | 16        | ND          |

Legend: □ D-Glc      ■ β-D-Galp-(1→2)-  
 ▲ α-D-Xylp-(1→6)-      □ β-D-Glcp-(1→4)-  
 ● α-L-Fucp-(1→2)-      ND, Not detectable

et al., 2002). Enzymes that catalyze the formation of the XyG backbone have not been cloned but probably are encoded by members of the cellulose synthase-like superfamily (Richmond and Somerville, 2001).

Screening of chemically mutagenized *Arabidopsis* plants for abnormal cell wall monosaccharide composition yielded two nonallelic mutant lines (*mur2* and *mur3*) that have an ~50% reduction in cell wall fucose content (Reiter et al., 1997). The *mur2* plants were shown recently to contain a missense mutation in the fucosyltransferase AtFUT1 that causes a loss of enzyme function and an absence of XyG fucosylation (Vanzin et al., 2002). We report here that the *Arabidopsis mur3* defect results in a failure of attachment of the Gal residue on the third xylosyl unit within the XXXG core structure. This failure severely alters the XyG structure in two ways. First, the  $\alpha$ -L-Fuc-(1→2)- $\beta$ -D-Gal-(1→2)- side group, which is considered important for XyG binding to cellulose, is completely absent. Second, galactosylation at the second xylose residue is enhanced. We also report that the *MUR3* gene encodes a residue-specific XyG galactosyltransferase that is homologous with the glucuronosyltransferase domain of exostosins. These animal enzymes catalyze the synthesis of heparan sulfate, a glycosaminoglycan involved in cell adhesion and intercellular communication pathways. This finding establishes an evolutionary relationship between the synthesis of two important

extracellular matrix components involved in the development of plants and animals.

## RESULTS AND DISCUSSION

### *mur3* Plants Have Severely Altered XyG

To determine which polysaccharide(s) are affected by the *mur3* mutation, cell wall material from the leaves of wild-type and *mur3* plants was fractionated into pectin- and XyG-enriched fractions. Monosaccharide composition analysis revealed a >90% reduction of fucose content in the 4 M KOH fraction of *mur3*, which typically contains most of the XyG solubilized from cell wall material (Figure 1A). A strong reduction in fucose content also was observed in the 1 M KOH fraction of *mur3*, which con-

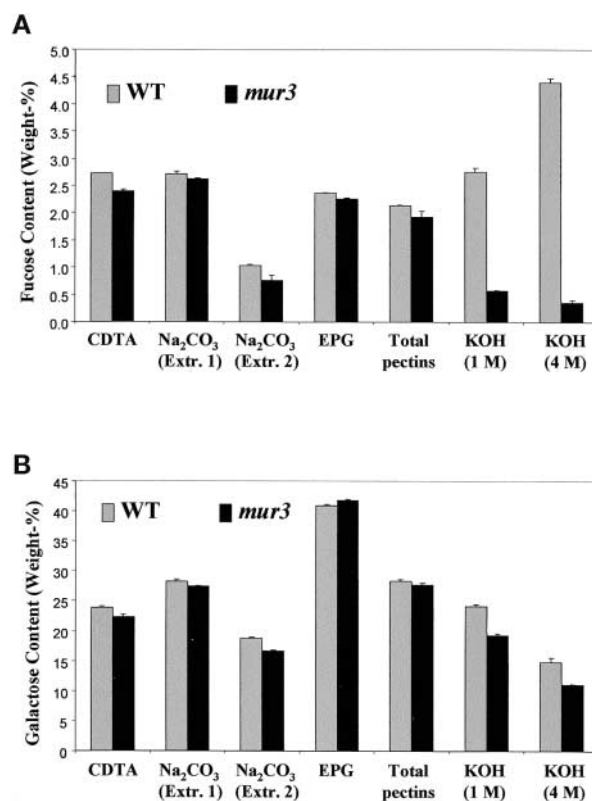


**Figure 1.** Fractionation of Cell Wall Material Reveals That the *mur3* Mutation Specifically Affects Polymers Extracted by Molar Concentrations of Alkali.

Cell wall material from wild-type (WT) and mutant plants was purified as described (Vanzin et al., 2002) except that a starch extraction step with 90% DMSO (Carpita and Kanabus, 1987) was included. The relative weight (%) of fucose (**A**) and galactose (**B**) are shown for the four pectin-enriched fractions (cyclohexane diamine tetraacetic acid [CDTA] extractable, ice-cold Na<sub>2</sub>CO<sub>3</sub> extractable [Extr. 1], room temperature Na<sub>2</sub>CO<sub>3</sub> extractable [Extr. 2], and endopolygalacturonase [EPG] released), pooled pectic material (total pectin), and two fractions composed primarily of xylans and XyGs (1 M KOH and 4 M KOH extracts). Monosaccharides were quantified by gas-liquid chromatography of alditol acetates as described previously (Reiter et al., 1993).

tains xylans, XyG, and some pectins. In addition to fucose, the 1 M KOH and 4 M KOH fractions also showed significant reduction of their galactose contents (Figure 1B). No significant changes in the relative percentages of fucose and galactose were observed in fractions containing primarily pectic material (Figure 1). Furthermore, the relative abundances of all other monosaccharides investigated (L-rhamnose, L-arabinose, D-xylose, D-mannose, and D-glucose) were not significantly different between the wild-type and *mur3* samples (data not shown). This experiment indicated that the *mur3* mutation affects the monosaccharide composition of XyG. Fractionation of cell wall material from roots, flowers, and inflorescence stems of wild-type and *mur3* plants yielded similar results (data not shown), indicating that the change in XyG structure affected all major plant organs.

To determine the structural alterations in *mur3* XyG in more detail, cell wall polysaccharides in the 1 M KOH and 4 M KOH

fractions were digested with an endo- $\beta$ -D-glucanase from *T. viride* that specifically cleaves the XyG backbone at the unsubstituted glucose residues, to yield XXXG building blocks and their galactosylated and fucosylated derivatives (Table 1). Separation and quantitation of these oligomers derived from *mur3* XyG by high-performance anion-exchange chromatography (HPAEC)-pulsed-amperometric detection gave only XXXG and its monogalactosylated derivative XLXG but none of the other four oligomers that normally are present in wild-type XyG (Figure 2A, Table 1).

To confirm these results independently, the endoglucanase digests were analyzed by electrospray tandem mass spectrometry (MS-MS), which yields the molecular masses of individual oligosaccharides. This method revealed that *mur3* XyG contained only oligomers of mass-to-charge ratio ( $m/z$ ) 1085 and  $m/z$  1247 (Figure 2B). The latter compound could be either XLXG or XXLG or a mixture of the two oligosaccharides, which

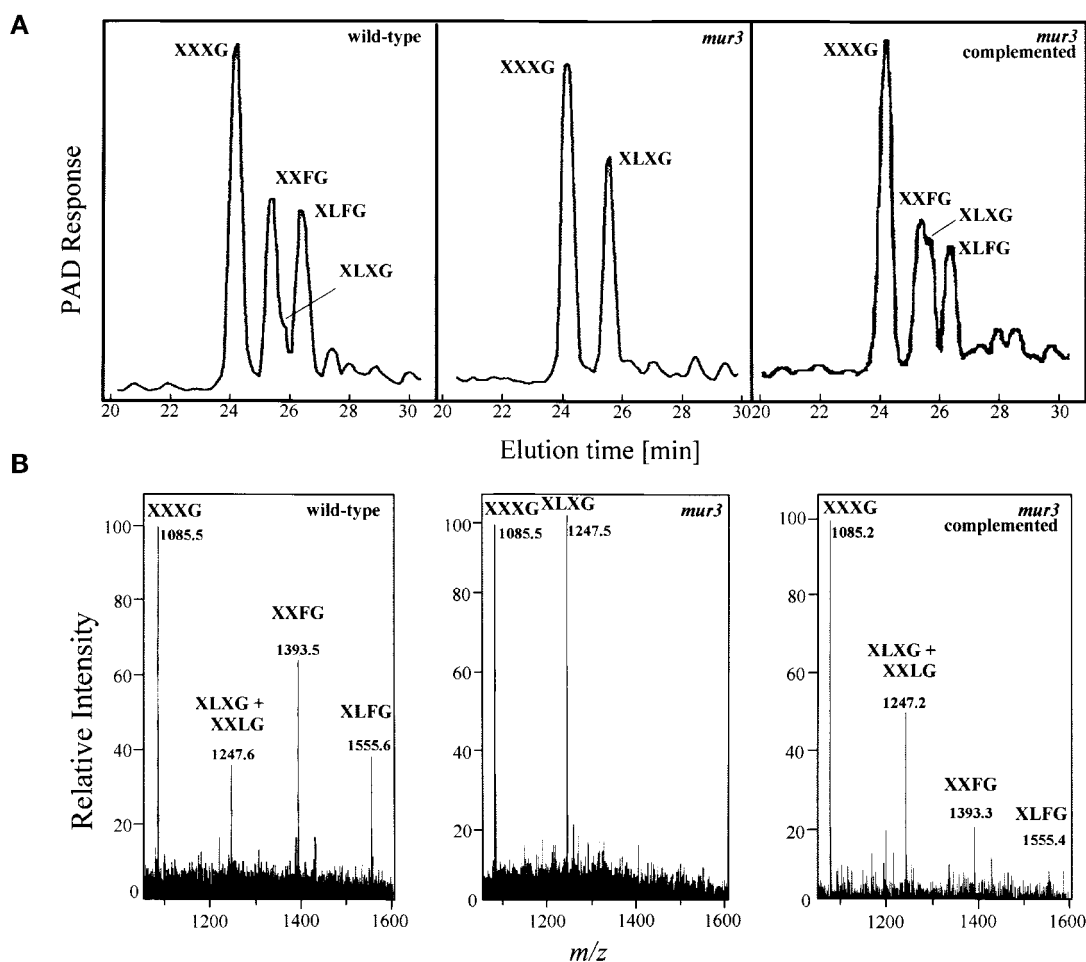


**Figure 2.** XyG from *mur3* Plants Lacks Galactose on the Third Xylose Moiety within the XXXG Core Structure.

**(A)** HPAEC separations of XyG oligosaccharides from wild-type and *mur3* plants and *mur3* plants transformed with a wild-type copy of the *MUR3* gene (*mur3* complemented). Isolation of XyG from *Arabidopsis* plants, digestion with endoglucanase, and HPAEC analysis were performed as described previously (Vanzin et al., 2002). Note that the complemented *mur3* plants represent a population that segregates for the *MUR3* transgene. PAD, pulsed-amperometric detection.

**(B)** Electrospray MS results on the same oligosaccharide preparations shown in **(A)**.

have identical masses. These oligomers can be differentiated by MS-MS through a predictable fragmentation of the  $m/z$  1247 ion (Vanzin et al., 2002).

Among the several expected fragmentations for XLXG, cleavage in the middle of the oligomer yielded a characteristic  $m/z$  773 ion from the nonreducing end, whereas a similar cleavage of XXLG oligomer produced a  $m/z$  659 ion from the reducing end (Figure 3). Thus, comparison of the ratios of  $m/z$  659 to  $m/z$  773 from the  $m/z$  1247 ions gives the relative abundance of each oligomer. Whereas XyG from *mur2* plants contained both of these diagnostic ions, indicating that both XLXG and XXLG were present (Vanzin et al., 2002),  $m/z$  1247 of *mur3* XyG oligomers contained only  $m/z$  773, indicating that only XLXG was present (Figure 3). These results are in agreement with the HPAEC-pulsed-amperometric detection data and indicate that *mur3* XyG lacks the entire  $\alpha$ -L-Fuc-(1 $\rightarrow$ 2)- $\beta$ -D-Gal side chain that is the hallmark of fucogalactoxyloglucans found in most flowering plants. Quantitation of the various XyG-derived oligomers from wild-type and *mur3* plants indicated that galactosylation at the central xylose residue within the XXXG core structure was enhanced strongly in *Arabidopsis mur3* (Table 1), which may compensate for the loss of the  $\alpha$ -L-Fuc-(1 $\rightarrow$ 2)- $\beta$ -D-Gal side chain (see below).

### Phenotypic Characterization of *mur3* Plants

Despite a severely altered XyG from which the fucosylated disaccharide side chain is completely absent, *mur3* plants are visibly indistinguishable from wild-type plants except for a collapsed appearance of trichome papillae (Figure 4), which was more severe than a similar phenotype in *Arabidopsis mur2*

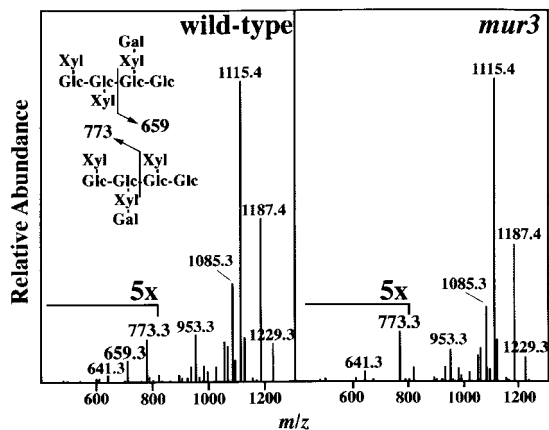


**Figure 3.** Comparison of the MS-MS Spectra of  $m/z$  1247 from Singly Galactosylated XyG Oligomers from Wild-Type and *mur3* Leaves Taken at 32 Days.

The inset shows the predicted primary fragmentation patterns that give  $m/z$  659 and  $m/z$  773 from XXLG and XLXG, respectively. To obtain these spectra, the  $m/z$  1247 ions were trapped after electrospray MS and helium was introduced as the collision gas during collisionally activated decomposition (MS-MS) experiments. The relative response factors for  $m/z$  659 and  $m/z$  773 were estimated from fragmentation of  $m/z$  1409 corresponding to XLLG and used for quantitation of the molar amounts of XXLG and XLXG listed in Table 1.

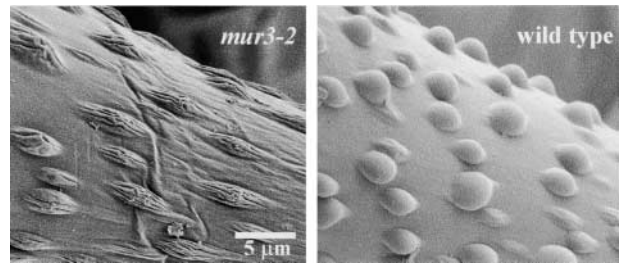


**Figure 4.** Scanning Electron Micrographs of the Surfaces of Trichomes from *mur3* and Wild-Type Plants.

Mature rosette leaves were fixed and visualized as described (Vanzin et al., 2002).

(Vanzin et al., 2002). Because the trisaccharide side chain in XyGs is believed to be important for hydrogen bonding to cellulose, we determined the force needed to break elongating *mur3* inflorescence stems (Reiter et al., 1993) but found no significant difference between wild-type and mutant plants (break force of  $10.7 \pm 2.9$  Newtons/mg cell wall material for wild type and  $10.3 \pm 2.8$  Newtons/mg cell wall material for *mur3*). This finding suggests that the fucosylated side chain in XyGs is not as important for productive XyG-cellulose interactions as was thought previously. Nonetheless, the high abundance of XLXG in *mur3* XyG may compensate at least partially for the loss of the fucose-containing disaccharide. Results from computer modeling studies suggest that the XLXG oligomer is similarly effective in straightening the XyG backbone as the XXFG building block (Levy et al., 1997). Accordingly, the high abundance of XLXG in *mur3* plants may reflect a compensatory mechanism in XyG biosynthesis to maintain strong XyG-cellulose interactions.

In contrast to bioassay results from pea stem segments (York et al., 1984; Zablackis et al., 1996), our genetic data indicate that the fucosylated side chain is not an essential modulator of elongation growth. This finding is in agreement with the absence of a growth defect in *Arabidopsis mur2*, which lacks the terminal fucose residue but contains XXLG and XLLG building blocks (Vanzin et al., 2002).

### Identification and Characterization of the *MUR3* Gene

Discovery of the altered XyG structure of *mur3* plants suggested that the *MUR3* gene encodes either a galactosyltransferase specific for the third xylose residue within the XXXG core structure or some factor that controls this enzymatic activity. To address this point, we used a positional cloning approach to identify the *MUR3* gene. After narrowing the map position of the *mur3* mutation to a region of 290 kb (Figure 5), hydropathy plots were used on all predicted coding regions to identify proteins with a single transmembrane domain at the N terminus, a structure typical of Golgi-localized glycosyltransferases. A single candidate gene was identified and shown to contain missense mutations in the two known *mur3* alleles (Figures 5 and 6). Transformation of *mur3* plants with a wild-type copy of this gene restored the normal galactosylation and fucosylation pattern of XyG (Figure 2, right trace), indicating that the *MUR3*

gene had been cloned. Based on the longest reading frame within the transcribed region and the GlimmerM gene-finder program (<http://www.tigr.org/software/glimmer/>), *MUR3* is predicted to encode a protein of 619 amino acids with a single transmembrane domain encompassing amino acid residues 32 to 54 (Figure 6). These results suggest that *MUR3* represents the structural gene for a XyG galactosyltransferase.

To verify the suspected function of the *MUR3* protein, we expressed the gene in *Pichia pastoris* and assayed crude extracts for XyG galactosyltransferase activities using *mur3*-derived XyG as the acceptor substrate and radiolabeled UDP-D-galactose as the donor substrate. Extracts from *MUR3*-expressing cells incorporated ~25-fold more radiolabel into ethanol-insoluble material than extracts from vector-transformed cells (Figure 7A). To characterize the structure of the reaction product, XyG from the enzyme assay was digested with endo- $\beta$ -D-glucanase, and products were separated by HPAEC. Incorporation of radiolabel was observed specifically at the position of XXLG using extracts from *MUR3*-expressing cells, whereas no labeling was observed with extracts from vector-transformed controls (Figure 7B). These data confirm that the *MUR3* gene encodes a glycosyltransferase that attaches D-galactose to the third xylose residue within the XXXG core structure.

### Transcription of the *MUR3* Gene

To determine the expression pattern of the *MUR3* gene, we used a semiquantitative reverse transcriptase-mediated PCR procedure on RNA from all major plant organs. This analysis in-

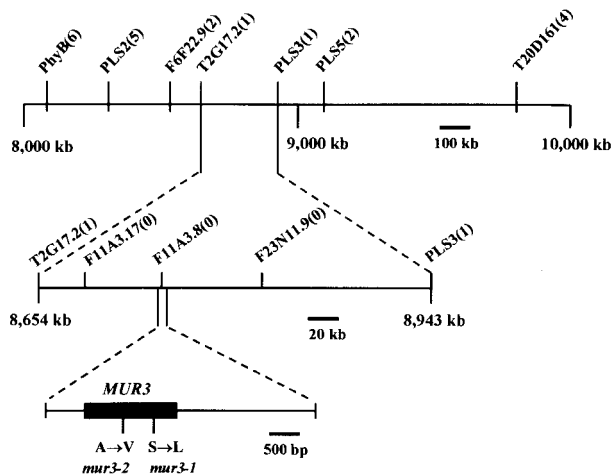


**Figure 5.** Identification of the *MUR3* Gene of Arabidopsis by Positional Cloning.

Physical map of the chromosomal region encompassing the *MUR3* gene as defined by high-resolution mapping. Map positions in kilobases refer to the distance from the top of chromosome II. The positions of molecular markers are indicated, with the number of recombinants given in parentheses [e.g., PLS2(5) denotes that five recombinant proteins were identified between molecular marker PLS2 and the *MUR3* gene]. The positions of missense mutations in the two *mur3* alleles are indicated.

```

1 MFPRVSMRRRSAEVSPTEPMEKNGKNGKQNTN
31 R[ICLLVALSLFFWALLLYFHFVVI]GTSNID
61 KQLQLQPSYAQSQPSSVSLRVDKFPPIEPAHA
91 APSKPPPKEPLVTIDKPIPPAPVANSSST
121 FKPPRIVESGKKQEFSEFIRALKTVDNKSDP
151 CGGKYIYVHNLPSKFNEDMLRDCKKLSLWT
181 NMCKFTTNAGLGPPLLENVEGVFSDEGWYAT
211 NQFAVDVIFSNRMKQYKCLTNDSSSLAAAF
241 VPFYAGFDIARYLWGYNISRRDAASLELVD

mur3-2: A→V
271 WLMKRPEWDIMRGKDHFLVAGRITWDFRRL
301 SEEETDWNKLLFLPAKNMSMLVVESSPW
331 NANDFGIPYPTYFHPAKDSEVFEWQDRMRN
361 LERKWLFSFAGAPRPDPNPKSIRGOIIDQCR
391 NSNVGKLECDFGSEKCHAPSSIMQMFQSS
421 LFCLQPQGDSYTRRSAFDSMLAGCIPVFFH

mur3-1: S→L
451 PGSAYTQYTWHLPKNYTTYSVFIPEDDVRK
481 RNISTEERLLQIPAKQVKIMRENVINLIPR
511 LIYADPRSELETQKDAFDVSVQAVIDKVT
541 LRKNMIEGRTEYDYFVEENSWKYALLEEGQ
571 REAGGHVWDPFFSKPKPGEDGSSDNGGTT
601 ISADAANKSWKSEQRDKTQ

```

**Figure 6.** Derived Amino Acid Sequence of the *MUR3* Protein.

The predicted transmembrane domain close to the N terminus is boxed, and the exostosin domain is underlined. Note that the C-terminal catalytic domain is predicted to reside within the Golgi lumen based on the transmembrane hidden Markov model algorithm (Krogh et al., 2001). Amino acid substitutions caused by the two known *mur3* mutations are indicated. Both of them are located within the exostosin-like domain.

dicated that *MUR3* mRNA is present in similar quantities throughout the plant (data not shown). Plants transgenic for a *MUR3*: $\beta$ -glucuronidase (*GUS*) construct were used to analyze *MUR3* transcription in more detail (Figure 8). *GUS* expression was observed in all major plant organs, in agreement with the reverse transcriptase-mediated PCR results. The gene expression data also are consistent with the absence of the  $\alpha$ -L-Fuc-(1 $\rightarrow$ 2)- $\beta$ -D-Gal-(1 $\rightarrow$ 2) side chain in XyG isolated from various parts of the plant, which suggests that there is no genetic redundancy in this aspect of XyG biosynthesis. Interestingly, the *MUR2* (*AtFUT1*) fucosyltransferase that completes the synthesis of this side chain also appears to be encoded by a single-copy gene (Vanzin et al., 2002), even though both *MUR2* and *MUR3* are members of large gene families (Sarria et al., 2001) (see below).

### Identification of *MUR3* Homologs in Plants and Animals

Searches of the dbEST database revealed putative *MUR3* orthologs with amino acid sequence identities of between 83 and 89% over 129 amino acids in many flowering plants, including important crop species such as alfalfa, tomato, and barley (Figure 9A). Within the Arabidopsis genome, we found 10 coding regions with sequence identities to *MUR3* of between 36 and 58% over 388 amino acids, plus 28 additional coding

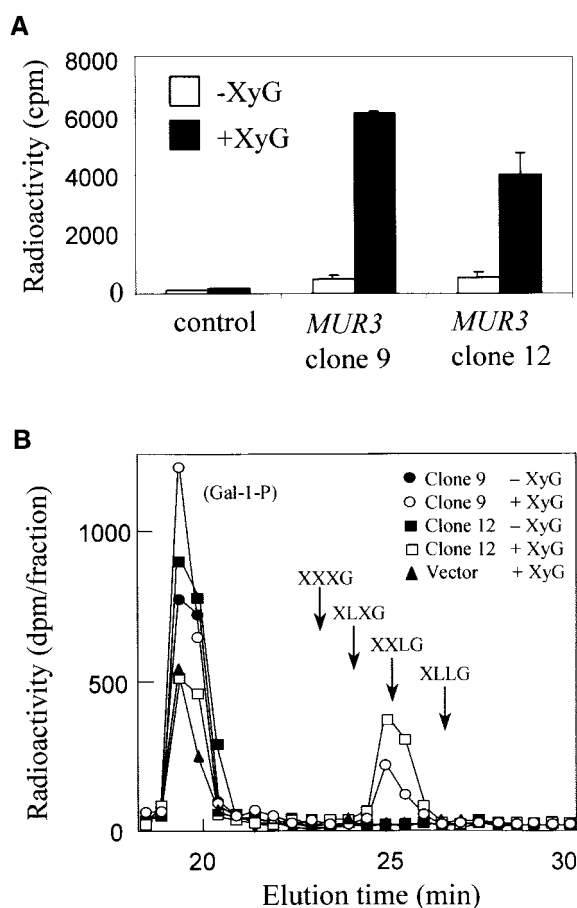


**Figure 7.** MUR3 Protein Expressed in *P. pastoris* Acts as a XyG Galactosyltransferase in Vitro.

**(A)** Incorporation of radiolabel from UDP-[U-<sup>14</sup>C]-D-galactose into *mur3*-derived XyG using crude extracts from two different *P. pastoris* clones expressing the MUR3 protein. Incubations in the absence of XyG and with extracts from *P. pastoris* cells transformed with vector alone were used as controls. The data shown are means of three samples  $\pm$  SD.

**(B)** Galactosyltransferase assay with *P. pastoris* cell extracts of two MUR3-expressing clones in the presence or absence of XyG purified from *mur3* leaves. XyG products of the reaction were digested with endoglucanase, and the resulting oligomers were separated by HPAEC (Vanzin et al., 2002). Radioactivity in individual fractions was quantified by liquid scintillation counting. The elution times of XyG oligosaccharides are indicated by arrows. Extracts from cells transformed with vector alone were used as a control. Galactose-1-P (Gal-1-P) appears in all reaction mixtures as a degradation product of unreacted UDP-galactose.

regions with lesser but easily recognizable sequence similarities to MUR3 (data not shown). Two of these coding regions (At5g61840 and At1g27440) show >89% sequence identity to a putative pectin glucuronosyltransferase from *Nicotiana glauca* (Iwai et al., 2002). The occurrence of transcribed MUR3 orthologs in solanaceous plants such as tomato and potato is of particular interest because members of this plant family show a replacement of D-galactose by L-arabinose within their XyG (Sims et al., 1996; York et al., 1996). L-Arabinose dif-

fers from D-galactose only by the absence of the C-6 hydroxymethyl group, suggesting that MUR3 homologs in solanaceous plants act as arabinosyltransferases rather than galactosyltransferases. The biochemical function of the MUR3 paralogs within the Arabidopsis genome is unknown at present, but at least one of them likely encodes a XyG galactosyltransferase that acts on the central xylose residue within the XXXG core structure to give the XLXG oligomer.

Searches of the Conserved Domain Database (Marchler-Bauer et al., 2002) (<http://www.ncbi.nlm.nih.gov/Structure/cdd/wrpsb.cgi>) indicated that all of these predicted proteins, including MUR3, contain domain pfam03016, which is representative of the glucuronosyltransferase domain of exostosins. These coding regions have been defined as glycosyltransferase family 47 by Henrissat et al. (2001) (see also <http://afmb.cnrs-mrs.fr/CAZY/>), but their function in plants had not been established. An alignment of MUR3 with representative members of these animal proteins is shown in Figure 9B.

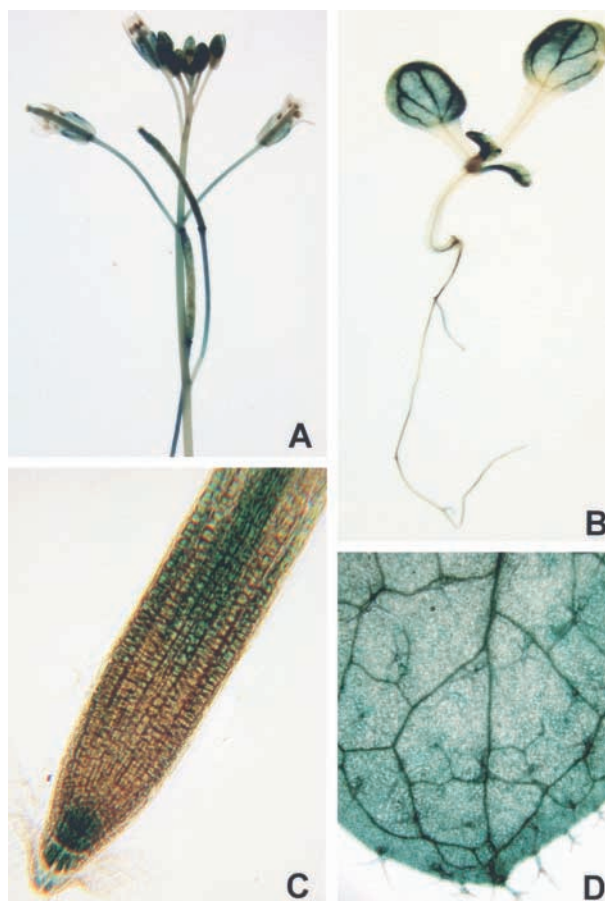


**Figure 8.** Expression of the GUS Reporter Gene under the Control of the MUR3 Promoter.

- (A)** Apical part of the inflorescence stem.  
**(B)** Young seedling with expanding primary leaves.  
**(C)** Tip of the primary root.  
**(D)** Apical part of the mature leaf.

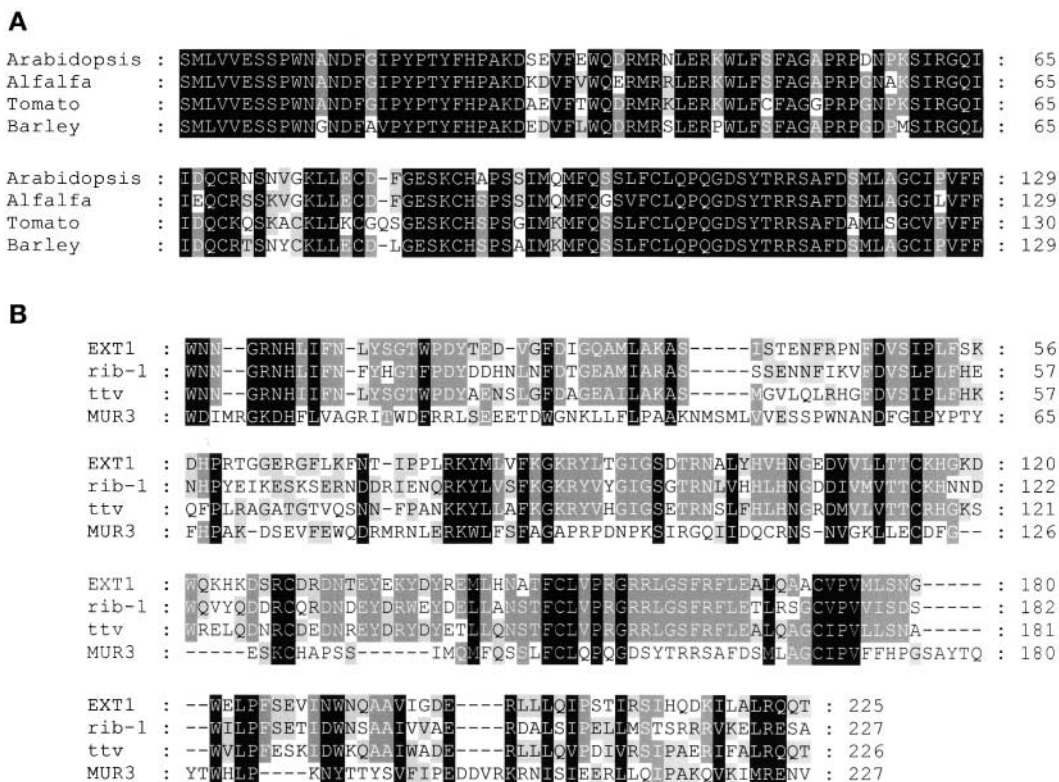


**Figure 9.** The *MUR3* Gene of Arabidopsis Has Orthologs in a Variety of Plant Species and Shows Sequence Similarities to Exostosins from Animals.

**(A)** Amino acid sequence alignment between *MUR3* (positions Ser-321 through Phe-449) and putative orthologs from crop species based on cDNA sequence entries in dbEST. The length of the alignment is limited by publicly available sequence data.

**(B)** Amino acid sequence alignment between *MUR3* (positions Trp-278 through Val-504) and MULTIPLE EXOSTOSES PROTEIN1 (EXT1) from human, the tout velu (*ttv*) gene product from *Drosophila melanogaster* that encodes an insect homolog of EXT1, and the *rib-1* gene product from *Caenorhabditis elegans* that is homologous with the glucuronosyltransferase domain of vertebrate exostosins. The protein segments selected for alignment represent conserved domain pfam03016 (exostosin family).

Exostosins were identified initially as tumor-suppressor genes required for normal bone growth in humans (Solomon, 1964). Later, they were shown to represent glycosyltransferases that catalyze the formation of heparan sulfate, an extracellular glycosaminoglycan that is synthesized initially as a linear chain of alternating GlcNAc and glucuronate residues and later modified in sulfation and sugar epimerization events (Esko and Selleck, 2002). Because heparan sulfate plays important roles in growth factor recognition and cell adhesion, defects in its synthesis are known to cause tumor formation in vertebrates and embryo lethality in *D. melanogaster* (Sugahara and Kitagawa, 2000). The conserved sequence motif between *MUR3*-like sequences from plants and exostosins from animals coincides with the (1→4)-β-D-glucuronosyltransferase domain (Wei et al., 2000) of the bifunctional animal enzymes (Figure 9B), whereas the putative GlcNAc transferase domain of the exostosins is absent from *MUR3*.

The sequence similarities between the plant galactosyltransferase in XyG synthesis and animal enzymes in the synthesis of glycosaminoglycans is unexpected considering that the donor and acceptor substrates are substantially different from each

other. The common denominator between the extracellular matrices of plants and animals is their prominent role in the growth and development of complex tissues and organs, which differentiates them from bacterial and fungal cell walls. It is interesting in this context that exostosin-like sequences appear to be absent from the genomes of the latter two groups of organisms.

## METHODS

### Plant Growth Conditions

*Arabidopsis thaliana* lines were grown at 23°C in ProMix BX potting mixture (Milikowski, Stafford Springs, CT) under continuous fluorescent light (60 to 70 μmol·m<sup>-2</sup>·s<sup>-1</sup>). In some experiments, nutrient agar plates (Haughn and Somerville, 1986) were used for axenic growth of seedlings.

### Cell Wall Fractionation and Analysis

The fractionation of cell wall material from wild-type, *mur3*, and complemented *mur3* plants was performed essentially as described (Vanzin et

al., 2002). Unless indicated otherwise, leaf material for cell wall fractionation was harvested from 3-week-old plants. All fractions were neutralized if necessary and dialyzed extensively against running deionized water and used either directly or as lyophilized material. The monosaccharide composition of cell wall polysaccharides was determined by gas-liquid chromatography of alditol acetates as described previously (Reiter et al., 1993).

### Determination of Xyloglucan Structure

Xyloglucans (XyGs) in the 1 M KOH and 4 M KOH extracts were digested with *Trichoderma viride* cellulase (Megazyme, Bray, Ireland), and the products were separated and detected by high-performance anion-exchange chromatography-pulsed-amperometric detection on a 0.4-cm-diameter × 25-cm-long PA-1 column (Dionex, Sunnyvale, CA) essentially as described (Vanzin et al., 2002). XyG oligomeric profiles were compared with XyG from tamarind seed (*Tamarindus indica*) XyG. Aliquots of the *T. viride* digestions also were subjected to electrospray mass spectrometry and tandem mass spectrometry of selected molecular masses as described previously (Vanzin et al., 2002).

### Genetic Mapping and Sequence Determination

To obtain a map position for the *mur3* locus, mutants in the Columbia genetic background were crossed to the Landsberg *erecta* ecotype, and plants from the F2 generation were analyzed for reductions in overall fucose content by gas-liquid chromatography of alditol acetates (Reiter et al., 1993). Mutants isolated during this screening procedure were allowed to self, and DNA was isolated from bulked F3 progeny. These DNA preparations then were used to determine the genotype (Columbia, Landsberg *erecta*, or heterozygous) of PCR-based molecular markers (Koniczny and Ausubel, 1993; Bell and Ecker, 1994). Marker information for fine-mapping purposes was taken from the TAIR World Wide Web site (<http://www.arabidopsis.org>). Nucleotide sequences were determined from both strands using the ABI Prism Big Dye Terminator Cycle Sequence Reaction Kit (Perkin-Elmer Applied Biosystems) and an ABI Prism 377 automated DNA sequencer.

### Genetic Complementation

A 3.53-kb fragment encompassing the *MUR3* coding region, 1.4 kb of upstream sequence, and 0.33 kb of downstream sequence was amplified from genomic Arabidopsis DNA, engineering a KpnI restriction site into the upstream primer and a Sall restriction site into the downstream primer. After cleavage of the PCR product with Sall and KpnI, it was cloned into the pCAMBIA1301 plant transformation vector (CAMBIA, Canberra, Australia) cleaved with the same two enzymes. Introduction of the recombinant plasmid into *Agrobacterium tumefaciens* GV3101/pMP90 and transformation of *mur3* plants via vacuum infiltration were performed as described (Bechtold et al., 1993).

### Analysis of Gene Expression

To obtain a *MUR3:GUS* reporter gene construct, a 2.5-kb fragment upstream of the *MUR3* coding region was amplified with TaKaRa EX Taq DNA Polymerase (PanVera, Madison, WI). The primer sequences for PCR were 5'-CAACAGAATTCTCTCCTCTCCTCTTGGTCCGGAA-3' (sense) and 5'-AACGTCATGGTCATTGGCTCTGTAGGAGAACTTCAG-3' (antisense). An EcoRI restriction site was engineered into the sense primer, and an NcoI restriction site was engineered into the reverse primer (underlined in the primer sequences). PCR products were ligated into the pCR2.1 TOPO vector and transformed into competent *Escherichia coli* TOP10F' cells (Invitrogen, Carlsbad, CA). After digestion of the plasmid

DNA with NcoI and EcoRI, the products were cloned in frame with the *uidA* reporter gene in pCAMBIA1301, giving pCAMBIA1301-MUR3.

To verify the structure of the construct, plasmid DNA was sequenced using the CEQ 2000 Dye Terminator Cycle Sequencing Kit and the CEQ 2000XL DNA Sequencer (Beckman, Fullerton, CA) with the sense primer described above and the vector-specific primer 5'-AAATAGATCAGT-TTAAAGAAAGATCAAAGCT-3' before *Agrobacterium*-mediated transformation into Arabidopsis according to the method of Bechtold et al. (1993).

Arabidopsis plants transformed with pCAMBIA1301-MUR3 were selected on hygromycin-containing medium essentially as described (Vanzin et al., 2002). At least 15 independent transformants were analyzed for GUS staining using a protocol adapted from Jefferson et al. (1987).

### Expression of the MUR3 Protein in *Pichia pastoris*

Recombinant MUR3 protein was produced using the *P. pastoris* expression system from Invitrogen. The *MUR3* sequence from amino acid positions 20 through 619 was amplified by PCR using the oligonucleotides 5'-CAACAGGTACCATGGAGAAGGGAAATGGAAAAATCAGAC-3' and 5'-CAACACCGCGGTGCTGTGTCTTATCTCTCTGCTCAC-3' (KpnI and SacII sites are underlined), ligated into the pCR2.1-TOPO vector, and transformed into competent *E. coli* TOP10F' cells (Invitrogen). After excision with KpnI and SacII, the *MUR3* coding region was cloned into the pPICZA expression vector to generate a fusion of *MUR3* with the *c-myc* and polyhistidine tags. After transformation into TOP10F' cells and verification of the insert sequence, the resulting plasmid, pPICZA-MUR3, was linearized with SacI and transformed into *P. pastoris* KM71 by electroporation as described by Burget et al. (2003). Transformants were selected on plates with yeast extract peptone dextrose sorbitol medium and zeocin (100 µg/mL).

To screen individual clones for high expression of the MUR3 protein, several transformants were plated on yeast extract peptone dextrose sorbitol plates with high concentrations of zeocin (200 and 500 µg/mL) and incubated for 2 days at 30°C. Several highly resistant colonies were used to inoculate 50 mL of buffered complex glycerol medium supplemented with 100 µg/mL zeocin in 250-mL flasks in a shaking incubator (28°C at 280 rpm) for 24 h until the OD<sub>600</sub> reached a value between 2 and 6. Cells were harvested by centrifugation and resuspended in buffered complex methanol medium to an OD<sub>600</sub> of 1.0. After 24 h, methanol was added to 0.5% (v/v) final concentration, and incubation was continued for another 24 h. Cells were harvested by centrifugation and stored at -80°C.

The preparation of crude extracts was performed as described by Burget et al. (2003). Assay reactions contained cell-free extract corresponding to 100 µg of total protein, 100 µg of XyG from *mur3* plants, 275,000 dpm of UDP-[U-<sup>14</sup>C]-D-galactose (250 mCi/mmol; American Radiolabeled Chemicals, St. Louis, MO), and 100 µL of 3× GalT assay buffer (40 mM Hepes/KOH, pH 6.2, 10 mM MgCl<sub>2</sub>, and 10 mM MnCl<sub>2</sub>) in a final volume of 300 µL. The reactions were terminated by incubation with proteinase K (500 µg/mL final concentration) and 0.5% SDS at 50°C for 1.5 h. After the addition of 1 mg of tamarind seed XyG as a carrier, ethanol was added to 80% final concentration, and the reaction mixture was incubated at room temperature for 4 h. After centrifugation, the XyG pellet was washed with 70% ethanol at 100°C and then dissolved in 300 µL of boiling water. One hundred microliters per reaction was used for liquid scintillation counting.

Upon request, all novel materials described in this article will be made available in a timely manner for noncommercial research purposes.

### Accession Numbers

Gene products discussed in this article have the following GenBank accession numbers: MUR3, AAD21751; rib-1, CAB61014; ttv, AAF58236; and EXT1, AAB62283.



## ACKNOWLEDGMENTS

We thank Michael Mølhoj for his help with the expression of *MUR3* in *P. pastoris*, Bruce Link for critical comments on the manuscript, and Karl Wood of the Purdue Mass Spectrometry facility for his assistance with electrospray MS. This work was supported by National Science Foundation Grant MCB-9728779 (to W.-D.R.) and a U.S. Department of Agriculture National Research Initiative Competitive Grants Program grant to N.C.C. This is journal paper 17,067 of the Purdue University Agricultural Experiment Station.

Received December 12, 2002; accepted April 23, 2003.

## REFERENCES

- Bechtold, N., Ellis, J., and Pelletier, G. (1993). In planta *Agrobacterium*-mediated gene transfer by infiltration of adult *Arabidopsis thaliana* plants. *C. R. Acad. Sci. Paris* **316**, 1194–1199.
- Bell, C.J., and Ecker, J.R. (1994). Assignment of 30 microsatellite loci to the linkage map of *Arabidopsis*. *Genomics* **19**, 137–144.
- Burget, E.G., Verma, R., Mølhoj, M., and Reiter, W.-D. (2003). The biosynthesis of L-arabinose in plants: Molecular cloning and characterization of a Golgi-localized UDP-D-xylose 4-epimerase encoded by the *MUR4* gene of *Arabidopsis*. *Plant Cell* **15**, 523–531.
- Carpita, N.C., and Gibeaut, D.M. (1993). Structural models of primary cell walls in flowering plants: Consistency of molecular structure with the physical properties of the walls during growth. *Plant J.* **3**, 1–30.
- Carpita, N.C., and Kanabus, J. (1987). Extraction of starch by dimethylsulfoxide and quantitation by enzymatic assay. *Anal. Biochem.* **161**, 132–139.
- Cosgrove, D.J. (2000). Loosening of plant cell walls by expansins. *Nature* **407**, 321–326.
- Esko, J.D., and Selleck, S.B. (2002). Order out of chaos: Assembly of ligand binding sites in heparan sulfate. *Annu. Rev. Biochem.* **71**, 435–471.
- Faik, A., Bar-Peled, M., DeRocher, A.E., Zeng, W.Q., Perrin, R.M., Wilkerson, C., Raikhel, N.V., and Keegstra, K. (2000). Biochemical characterization and molecular cloning of an  $\alpha$ -1,2-fucosyltransferase that catalyzes the last step of cell wall xyloglucan biosynthesis in pea. *J. Biol. Chem.* **275**, 15082–15089.
- Faik, A., Price, N.J., Raikhel, N.V., and Keegstra, K. (2002). An *Arabidopsis* gene encoding an  $\alpha$ -xylosyltransferase involved in xyloglucan biosynthesis. *Proc. Natl. Acad. Sci. USA* **99**, 7797–7802.
- Fry, S.C. (1994). Oligosaccharins as growth regulators. *Biochem. Soc. Symp.* **60**, 5–14.
- Fry, S.C., et al. (1993). An unambiguous nomenclature for xyloglucan-derived oligosaccharides. *Physiol. Plant.* **89**, 1–3.
- Haughn, G.W., and Somerville, C. (1986). Sulfonylurea-resistant mutants of *Arabidopsis thaliana*. *Mol. Gen. Genet.* **204**, 430–434.
- Henrissat, B., Coutinho, P.M., and Davies, G.J. (2001). A census of carbohydrate-active enzymes in the genome of *Arabidopsis thaliana*. *Plant Mol. Biol.* **47**, 55–72.
- Iwai, H., Masaoka, N., Ishii, T., and Satoh, S. (2002). A pectin glucuronosyltransferase gene is essential for intercellular attachment in the plant meristem. *Proc. Natl. Acad. Sci. USA* **99**, 16319–16324.
- Jefferson, R.A., Kavanagh, T.A., and Bevan, M.W. (1987). GUS fusions:  $\beta$ -Glucuronidase as a sensitive and versatile gene fusion marker in higher plants. *EMBO J.* **13**, 3901–3907.
- Konieczny, A., and Ausubel, F.M. (1993). A procedure for mapping *Arabidopsis* mutations using co-dominant ecotype-specific PCR-based markers. *Plant J.* **4**, 403–410.
- Krogh, A., Larsson, B., von Heijne, G., and Sonnhammer, E.L.L. (2001). Predicting transmembrane protein topology with a hidden Markov model: Application to complete genomes. *J. Mol. Biol.* **305**, 567–580.
- Levy, S., Maclachlan, G., and Staehelin, L.A. (1997). Xyloglucan sidechains modulate binding to cellulose during in vitro binding assays as predicted by conformational dynamics simulations. *Plant J.* **11**, 373–386.
- Levy, S., York, W.S., Stuike-Prill, R., Meyer, B., and Staehelin, L.A. (1991). Simulations of the static and dynamic molecular conformations of xyloglucan: The role of the fucosylated side-chain in surface-specific side-chain folding. *Plant J.* **1**, 195–215.
- Marchler-Bauer, A., Panchenko, A.R., Shoemaker, B.A., Thiessen, P.A., Geer, L.Y., and Bryant, S.H. (2002). CDD: A database of conserved domain alignments with links to domain three-dimensional structure. *Nucleic Acids Res.* **30**, 281–283.
- Nishitani, K. (1997). The role of endoxyloglucan transferase in the organization of plant cell walls. *Int. Rev. Cytol.* **173**, 157–206.
- Perrin, R.M., DeRocher, A.E., Bar-Peled, M., Zeng, W.Q., Norambuena, L., Orellana, A., Raikhel, N.V., and Keegstra, K. (1999). Xyloglucan fucosyltransferase, an enzyme involved in plant cell wall biosynthesis. *Science* **284**, 1976–1979.
- Purugganan, M.M., Braam, J., and Fry, S.C. (1997). The *Arabidopsis* TCH4 xyloglucan endotransglycosylase: Substrate specificity, pH optimum, and cold tolerance. *Plant Physiol.* **115**, 181–190.
- Reiter, W.-D., Chapple, C., and Somerville, C.R. (1993). Altered growth and cell walls in a fucose-deficient mutant of *Arabidopsis*. *Science* **261**, 1032–1035.
- Reiter, W.-D., Chapple, C., and Somerville, C.R. (1997). Mutants of *Arabidopsis thaliana* with altered cell wall polysaccharide composition. *Plant J.* **12**, 335–345.
- Richmond, T.A., and Somerville, C.R. (2001). Integrative approaches to determining Csl function. *Plant Mol. Biol.* **47**, 131–143.
- Sarria, R., Wagner, T.A., O'Neill, M.A., Faik, A., Wilkerson, C.G., Keegstra, K., and Raikhel, N.V. (2001). Characterization of a family of *Arabidopsis* genes related to xyloglucan fucosyltransferase 1. *Plant Physiol.* **127**, 1595–1606.
- Sims, I.M., Munro, S.L.A., Currie, G., Craik, D., and Bacic, A. (1996). Structural characterization of xyloglucan secreted by suspension-cultured cells of *Nicotiana plumbaginifolia*. *Carbohydr. Res.* **293**, 147–172.
- Solomon, L. (1964). Hereditary multiple exostosis. *Am. J. Hum. Genet.* **16**, 351–363.
- Sugahara, K., and Kitagawa, H. (2000). Recent advances in the study of the biosynthesis and functions of sulfated glycosaminoglycans. *Curr. Opin. Struct. Biol.* **10**, 518–527.
- Vanzin, G.F., Madson, M., Carpita, N.C., Raikhel, N.V., Keegstra, K., and Reiter, W.-D. (2002). The *mur2* mutant of *Arabidopsis thaliana* lacks fucosylated xyloglucan because of a lesion in fucosyltransferase AtFUT1. *Proc. Natl. Acad. Sci. USA* **99**, 3340–3345.
- Wei, G., Bai, X.M., Gabb, M.M.G., Bame, K.J., Koshy, T.I., Spear, P.G., and Esko, J.D. (2000). Location of the glucuronosyltransferase domain in the heparan sulfate copolymerase EXT1 by analysis of Chinese hamster ovary cell mutants. *J. Biol. Chem.* **275**, 27733–27740.
- York, W.S., Darvill, A.G., and Albersheim, P. (1984). Inhibition of 2,4-dichlorophenoxyacetic acid-stimulated elongation of pea stem segments by a xyloglucan oligosaccharide. *Plant Physiol.* **75**, 295–297.
- York, W.S., Kolli, V.S.K., Orlando, R., Albersheim, P., and Darvill, A.G. (1996). The structures of arabinoxyloglucans produced by solanaceous plants. *Carbohydr. Res.* **285**, 99–128.
- Zablackis, E., York, W.S., Pauly, M., Hantus, S., Reiter, W.-D., Chapple, C.C.S., Albersheim, P., and Darvill, A. (1996). Substitution of L-fucose by L-galactose in cell walls of *Arabidopsis mur1*. *Science* **272**, 1808–1810.

**The *MUR3* Gene of *Arabidopsis* Encodes a Xyloglucan Galactosyltransferase That Is Evolutionarily Related to Animal Exostosins**

Michael Madson, Christophe Dunand, Xuemei Li, Rajeev Verma, Gary F. Vanzin, Jeffrey Caplan, Douglas A. Shoue, Nicholas C. Carpita and Wolf-Dieter Reiter  
*Plant Cell* 2003;15;1662-1670; originally published online June 5, 2003;  
DOI 10.1105/tpc.009837

This information is current as of November 27, 2020

|                                 |   |
|---------------------------------|---|
| <b>References</b>               | This article cites 35 articles, 12 of which can be accessed free at:<br><a href="/content/15/7/1662.full.html#ref-list-1">/content/15/7/1662.full.html#ref-list-1</a>   |
| <b>Permissions</b>              | <a href="https://www.copyright.com/ccc/openurl.do?sid=pd_hw1532298X&amp;issn=1532298X&amp;WT.mc_id=pd_hw1532298X">https://www.copyright.com/ccc/openurl.do?sid=pd_hw1532298X&amp;issn=1532298X&amp;WT.mc_id=pd_hw1532298X</a> |
| <b>eTOCs</b>                    | Sign up for eTOCs at:<br><a href="http://www.plantcell.org/cgi/alerts/ctmain">http://www.plantcell.org/cgi/alerts/ctmain</a>  |
| <b>CiteTrack Alerts</b>         | Sign up for CiteTrack Alerts at:<br><a href="http://www.plantcell.org/cgi/alerts/ctmain">http://www.plantcell.org/cgi/alerts/ctmain</a>   |
| <b>Subscription Information</b> | Subscription Information for <i>The Plant Cell</i> and <i>Plant Physiology</i> is available at:<br><a href="http://www.aspb.org/publications/subscriptions.cfm">http://www.aspb.org/publications/subscriptions.cfm</a>        |